JOURNAL OF AIRCRAFT
Vol. 43, No. 6, November–December 2006

Fan Noise Reduction with Increased Bypass Nozzle Area

Richard P. Woodward,* Christopher E. Hughes,† and Gary G. Podboy*
NASA Glenn Research Center, Cleveland, Ohio 44135

DOI: 10.2514/1.19359

A model turbofan was tested in the NASA Glenn 9- by 15-ft low speed wind tunnel to explore far-field acoustic effects of a variable area bypass nozzle using three fixed nozzle flows. The baseline nozzle was sized to produce maximum stage performance at cruise condition. However, wind tunnel testing is conducted near sea level condition. Therefore, to simulate and obtain performance at other operating conditions, two additional nozzles were tested—one with +5% increase in weight flow (+5.4% area increase), sized to simulate the performance at the stage design point (takeoff) condition, and the other with a +7.5% increase in weight flow (+10.9% area increase) sized for maximum weight flow at sea level condition. Measured acoustic benefits with increased nozzle area showed effective perceived noise level reductions of 2 or more dB (for a 1500 ft fan flyover with a 3.35 scale factor) while the stage thrust actually increased by 2 to 3%. Noise reductions, principally in the level of broadband noise, were observed everywhere in the far field. Laser Doppler velocimetry measurements downstream of the rotor showed that the total turbulent velocity decreased with increasing nozzle flow, which may explain the reduced rotor broadband noise levels.

I. Introduction

FAN noise tests reported in the literature have shown the potential for significant reductions in broadband noise levels associated with a variable area bypass nozzle flow (increased area or reduced throttling). Woodward et al. [1] presents results for a 6 ft diam fan which was tested in the NASA Glenn (formerly NASA Lewis) Quiet Fan Facility. The fan, designated QF-6, had a relatively low 1.2 stage pressure ratio and design rotor tip speed (750 ft/s) and represented early 1970s turbofan design. There was no consideration of inflow turbulence control for this test. However, results for QF-6 showed that the far-field broadband sound pressure level (SPL) decreased by 4 dB or more as the stage exit nozzle area increased from 95 to 105% of the design. The overall sound power level (OAPWL) showed a similar decrease as the nozzle area was increased. This was accompanied with an increase in the stage adiabatic efficiency with increased nozzle area. This noise reduction with increased bypass nozzle area was repeated for another fan [2] (QF-2) tested in the NASA Quiet Fan Facility. QF-2 was a 1.5 stage pressure ratio, 1107 ft/s tip speed fan which likewise represented 1970 turbofan technology.

Woodward, Glaser, and Gliebe [3,4] presented forward arc acoustic results for fans statically tested in anechoic facilities using inflow control devices to minimize inlet turbulence. Acoustic results for these two tests also suggested that broadband noise levels may be reduced as the stage flow is increased through reduced downstream throttling (analogous to increased bypass nozzle area). Ginder and Newby [5] considered forward arc acoustic results for several fans statically tested in an anechoic facility with inflow control as well as the QF-6 results of [1]. They concluded that the fan stage broadband noise levels were related to changes in the rotor leading edge incidence, which changed with the stage nozzle area or flow. They concluded that the maximum fan stage broadband noise level changed by about 1.7 dB per degree change in the rotor incidence angle.

Reductions in turbofan noise levels are an important component of current efforts to reduce overall jet aircraft noise levels. The NASA Glenn fan broadband source diagnostic tests (SDT2) provided the opportunity to reevaluate the potential for fan stage broadband noise reduction for a current technology turbofan. The test facility environment enabled taking far-field acoustic data in an anechoic, low turbulence wind tunnel environment simulating takeoff/approach conditions.

This paper presents SDT2 results showing the potential for fan noise reduction with a variable area bypass nozzle. The SDT2 tests were conducted in the NASA Glenn 9 × 15-ft low speed wind tunnel (9 × 15 LSWT). References [6–11] present earlier results from this test series. The 9 × 15 LSWT provides a low turbulence, anechoic test environment for fan aeroacoustic tests [12–14]. Three fixed-area nozzles were used in this study. The baseline nozzle was sized for sea level takeoff condition. Two additional nozzles were also tested, one with a +5% increase in flow, corresponding to a +5.4% increase in area [sized for design point (takeoff) condition at 100% rotor design speed] and a +7.5% increase in flow, corresponding to a +10.9% increase in area (sized for maximum flow with a fixed nozzle at sea level condition). Measured acoustic benefits with increased nozzle area were very encouraging, showing flyover effective perceived noise level (EPNL) reductions of 2 or more dB (for a 1500 ft fan flyover), whereas the stage thrust typically increased by several percentage points. EPNLs were calculated with a 3.35 scale factor which is representative of a typical midsize engine. These noise reduction benefits were primarily for the broadband noise and were evident throughout the range of measured sideline angles. Concurrent laser Doppler velocimetry measurements taken between the rotor and the stator showed a decrease in total turbulent velocity with increased nozzle area, which could help explain the observed reduction in broadband noise with the more open nozzles. Additional results for the SDT2 increased nozzle area are presented in [15,16].

II. Description of Fan Test

A. Research Hardware

Results presented herein are for the SDT2 fan stage with the baseline, R4 rotor and baseline radial stator (Table 1). The R4 rotor had 22 blades and a nominal 22 in. diameter. The baseline radial stator had 54 blades and thus was cutoff for the fundamental rotor-stator interaction tone [17]. Figure 1 is a cross sectional sketch of the research fan stage with the R4 rotor and baseline stator and a photograph of the fan and stator without the nacelle installed in the wind tunnel. The rotor-stator spacing is a nominal 2.5 axial rotor chords.

Received 8 August 2005; revision received 2 December 2005; accepted for publication 16 January 2006.

*Acoustics Branch MS 54-3, 21000 Brookpark Road. Senior Member, AIAA.
†Acoustics Branch MS 54-3, 21000 Brookpark Road.

Table 1 SDT2 research fan stage design parameters

R4 rotor	
No. of blades	22
Tip diameter, in.	22
Inlet radius ratio	0.30
Corrected design speed, RPM	12,657
Design tip speed, ft/s	1,215
Corrected weight flow, lbm/s	100.5
Specific flow, lbm/s-ft^2	41.8
Stage pressure ratio	1.47

Baseline stator			
No. vanes	L. E. sweep	Aspect ratio	Solidity
54	0^0	3.51	1.52

Three fixed-area fan nozzles were tested. Each nozzle was designed to reach a specific operating condition on the rotor and stage operating maps. The fixed-area, "flight-type" engine nozzles are typically sized to maximize engine efficiency cruise conditions at cruise altitude. The three bypass nozzles used for this test were designed as follows: 1) a minimum flow-baseline nozzle, used as the nozzle design for all acoustic testing and designed to achieve minimum stator pressure losses and maximum thrust at takeoff conditions without sacrificing cruise operating performance; 2) a design point nozzle, which allowed a +5% increase in weight flow with a +5.4% increase in nozzle area compared to the baseline nozzle over the fan stage operating range in order to achieve the design point fan weight flow and pressure ratio conditions at 100% corrected rotor design speed; and 3) a high flow nozzle, which allowed the maximum weight flow possible through the fan at sea level conditions or +7.5% above the baseline nozzle with a 10.9% increase in nozzle area. The purpose was to determine the effect of reduced rotor blade loading and increased nozzle exit velocity on the fan stage performance and acoustics over a range of operating conditions that would be seen for this particular design in an engine application. Each of the bypass nozzles allowed a different fan stage operating line at sea level conditions. A sketch of the three bypass nozzle geometries is shown in Fig. 2.

B. Anechoic Wind Tunnel and Acoustic Instrumentation

The tunnel test section walls, floor, and ceiling have acoustic treatment to produce an anechoic test environment. Sideline acoustic data were acquired with a computer-controlled translating microphone probe and with three aft microphone assemblies mounted to the tunnel floor. The translating microphone probe acquired data at 48 sideline geometric angles from 27.2 to 134.6 deg relative to the fan rotor plane. The probe traverse was 89 in. from the fan rotational axis (about four fan diameters). The three fixed microphone assemblies were mounted at the downstream traverse position to acquire aft acoustic data at geometric angles of 140, 150, and 160 deg. Data were also acquired with an acoustic barrier wall installed adjacent to the fan which effectively blocked aft-radiated fan noise. Figure 3 is a photograph of the installed research fan with the acoustic barrier wall in place. Downstream fixed microphones were not used with the wall installed because of acoustic blockage. The sideline traversing microphone probe may be seen to the left of the research fan. The acoustic data were acquired through a digital computer system and stored for postrun analysis.

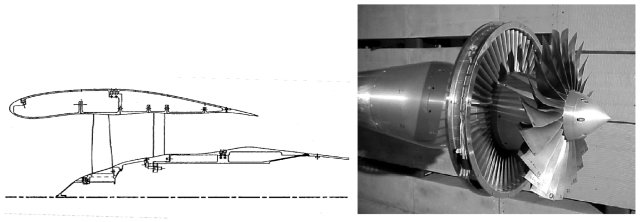

Fig. 1 Cross sectional sketch and photograph of the test fan stage with R4 rotor and baseline stator.

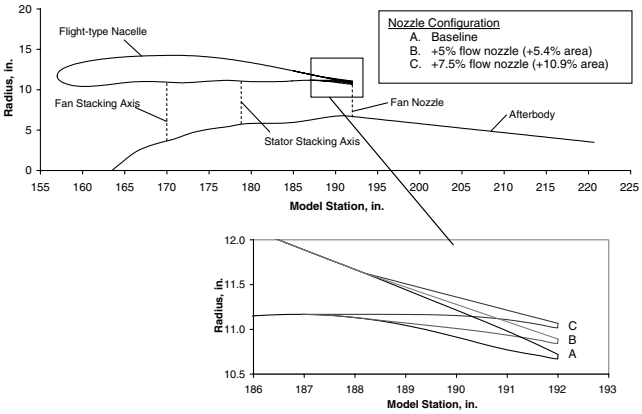

Fig. 2 Sketch of fan nozzle geometry configurations.

Fig. 3 Photograph of the research fan with the acoustic barrier wall in place.

III. Results and Discussion

A. Aerodynamic Performance

Test results indicate that there was an increase in stage thrust with increased bypass nozzle area at most fan speeds. However, aerodynamic data taken concurrently with acoustic testing were limited to rotor and stator assembly thrust and torque due to the need for clean airflow within the model (removal of protruding measuring rakes, etc.). Therefore, the thrust values presented herein are from rotating and static force balance measurements made during acoustic testing. Thrust values are available for the rotor and for the stator/nacelle/afterbody assembly, which includes the stators, flight nacelle, and aft inner bypass flowpath representing the outer boundary of the simulated core hardware downstream of the bypass nozzle. Fan stage thrust measurements are a combination of the rotor thrust from rotating force balance measurements and stator/nacelle/afterbody thrust from static force balance measurements obtained simultaneously during testing. Results from these force balance measurements provided valid rotor and stage thrust values at tunnel test conditions.

Figure 4 is a fan operating map showing performance lines for the three nozzle areas. The fan was operating in an acceptable region of the fan map except for the most open nozzle at 95 and 100% design speed which was into the choke region.

Figure 5 shows a consistent increase in stage thrust with increased nozzle area at all rotor test speeds, except for the high flow nozzle at the highest rotor speeds. The accuracy of the measured thrust is ±10 lbf, or ±0.25% of the full scale measurement range (4000 lbf)

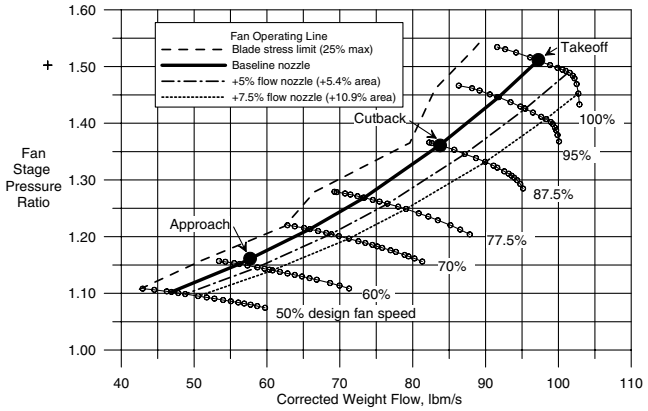

Fig. 4 Fan operating map showing the three nozzle flow areas.

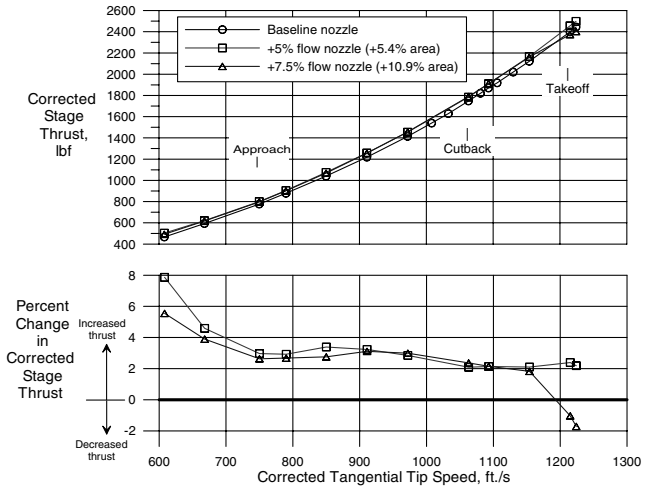

Fig. 5 Corrected stage thrust as a function of corrected tangential tip speed for three bypass nozzle areas.

of the combined balances. A description of the technique used for force balance performance measurement can be found in [18]. Also shown in Fig. 5 is the percent change in corrected stage thrust for the three nozzle flows. These delta thrust values were obtained by inspecting the total thrust levels at particular rotor tip speeds. Stage thrust levels for the +5% flow nozzle were about 3% higher than for the reference nozzle at approach rotor speed, and slightly more than 2% higher at cutback and takeoff rotor speed. Even higher thrust levels are seen for the +7.5% flow nozzle at approach and cutback rotor speeds. However, thrust levels for this nozzle area drop off toward takeoff (design) rotor speed, indicating degrading stage flow conditions for this nozzle at high rotor speeds. There was also an increase in the stage adiabatic efficiency with increased nozzle area [16] except for the most open nozzle near design fan speed. This result suggests that the rotor (but not the stator) is near choke for the most open nozzle at 100% design fan speed.

B. Acoustic Data Reduction

All of the fan acoustic data were acquired at 0.10 tunnel Mach, which is sufficient to cleanup ambient turblence [19]. Sideline data are presented in terms of emission angles. The emission angles are related to the geometric or observed angles by the relationship:

$$\Theta_{em} = \Theta_{geom} - \sin^{-1}(M_0 \sin \Theta_{geom})$$

where Θ_{em} and Θ_{geom} are, respectively, the emission and observed sideline angles, and M_0 is the test section Mach number. The observed angles for the sideline translating microphone probe are then 25 to 130 deg, and the three fixed microphones measure aft observed angles of 136, 147, and 158 deg. This angular range was

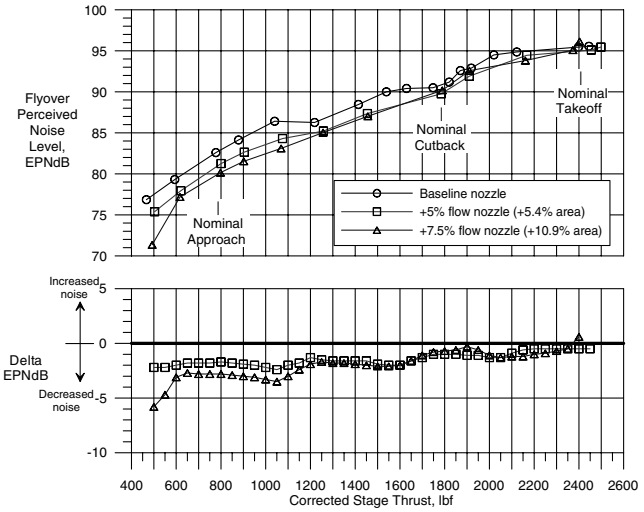

Fig. 6 Perceived noise level as a function of corrected stage thrust for three nozzle flows (1500 ft flyover and 3.35 scale factor).

sufficient to define the sideline noise profile for this aft-dominated fan for flyover EPNL calculations.

Digital acoustic data were processed as constant bandwidth spectra. Spectra were acquired and averaged at each translating probe or fixed mic position with 5.9 and 59 Hz bandwidths. These constant bandwidth spectra were electronically merged and used to generate 1/3-octave spectra. Sound power level (PWL) spectra were calculated from the SPL spectra assuming spherical symmetry through the range of sideline data acquisition. Possible noise contributions outside the sideline range were ignored.

C. Acoustic Results

Figure 6 shows the calculated EPNL for a 1500 ft "fan stage flyover" and a 3.35 scale factor. Figure 6 also shows the change in EPNL for the more open nozzles relative to that of the baseline, sea level design nozzle. These delta EPNLs were measured at constant thrust levels interpolated from the EPNL curves. Increasing the nozzle flow by 5% resulted in a 2 EPNdB noise reduction at rotor speeds up to cutback, and around a 1 EPNdB reduction at higher rotor speeds. Further increasing the nozzle flow to +7.5% gave noise reductions of about 3 EPNdB relative to the baseline nozzle at lower rotor speeds (near approach), although the noise reduction with the +7.5% flow nozzle was significantly higher at the lowest test fan speeds. Noise reductions for the +5 and +7.5% flow nozzles were about the same at high subsonic to design rotor speeds.

Figure 7 shows corresponding EPNL with the acoustic barrier wall in place (forward radiating noise). Interestingly, the inlet noise reduction with increased nozzle area is even greater than what was observed for the total fan stage without the barrier wall. Increasing the nozzle flow by +5% resulted in about a 2–4 EPNdB noise reduction at subsonic tip speeds, and up to 3 dB at design speed. Increasing the nozzle flow by +7.5% gave noise reductions from 3 to 7 EPNdB at subsonic tip speeds and as much as 7.5 dB at design rotor speed. The forward radiating noise levels near designated cutback (87.5% design fan speed, region of subsonic/supersonic tip flow transition) were mixed, showing additional noise for the +7.5% flow nozzle, and little change with the +5% flow nozzle.

The noise reductions associated with increased nozzle flow were primarily broadband noise. Figure 8 shows the sound power level spectra at the three fan stage rating conditions. Blade/vane numbers for this fan stage result in the fundamental rotor-stator interaction tone being essentially cut off at lower rotor speeds. Broadband noise levels at 61.7% design fan speed (designated approach condition) are up to 3 dB lower for the +5% flow nozzle and 6 dB lower for the +7.5% flow nozzle relative to noise levels for the baseline nozzle. The 2BPF interaction tone (cut-on) shows a small increase with increasing nozzle area. As will be shown with the laser Doppler

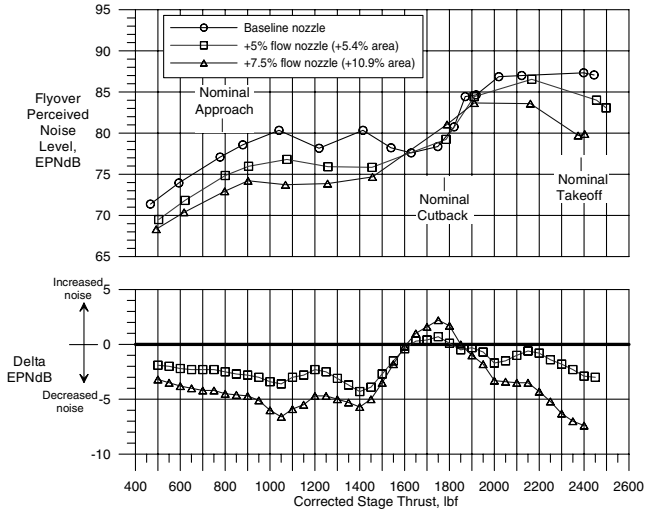

Fig. 7 Inlet radiating EPNL as a function of corrected stage thrust for three nozzle flows (acoustic barrier wall in place).

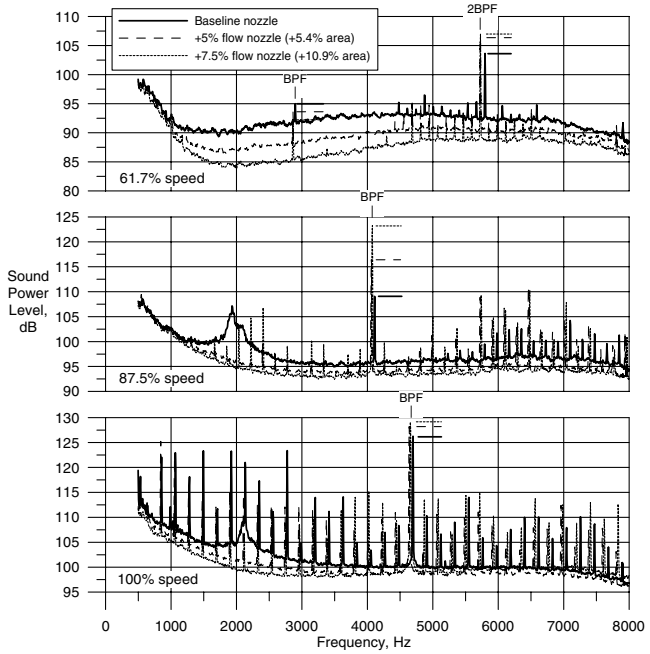

Fig. 8 Sound power level spectra at three fan speeds (5.9 Hz bandwidth, no barrier wall).

velocimeter results, there was an increase in rotor axial velocity and subsequent wake interaction with the stator with higher nozzle flow. A variable area nozzle provides a means to adjust the rotor inflow angle and thereby control blade losses and wakes with a resultant reduction in noise level.

There is a significant increase in BPF tone level with increasing nozzle flow at 87.5% design fan speed (designated cutback). Again, increasing the nozzle flow effectively increased the rotor relative velocity and wake strength. This is the speed region where the rotor relative velocity becomes transonic toward the tip, accompanied by the emergence of the "rotor-alone" tones and multiple pure tones (MPT, shaft order tones). The rotor-stator interaction tones (nBPF) include a contribution from the MPT noise. Small changes in the rotor tip relative velocity in this subsonic/supersonic region can generate significant changes in the rotor fundamental tone and multiple pure tones as evidenced in the spectra. There is a more modest reduction in broadband noise of about 2 dB with both increased flow nozzles at 87.5% design fan speed. The noise "hump" at about $1/2$ BPF for the baseline nozzle is unexplained.

The rotor tip relative velocity is well into the supersonic range at design fan speed (designated takeoff). Consequently the multiple pure tones are well established regardless of nozzle flow changes. The BPF tone level shows a small increase with increasing nozzle flow at design speed with a corresponding small decrease in broadband noise level.

Observed noise reductions with increased nozzle flow typically occurred at all measured sideline angles. Figures 9–11 show 59 Hz bandwidth sound pressure level directivities for the fundamental (BPF) rotor tone and representative broadband noise at, respectively, 61.7, 87.5, and 100% design fan speed. At 61.7% design fan speed the noise level at the cutoff BPF frequency (Fig. 9) was reduced by about 2 dB with the +5% flow nozzle, and about 5 dB with the +7.5% flow nozzle. The representative broadband directivities between BPF and 2BPF in Fig. 9 again show a nominal 2 dB

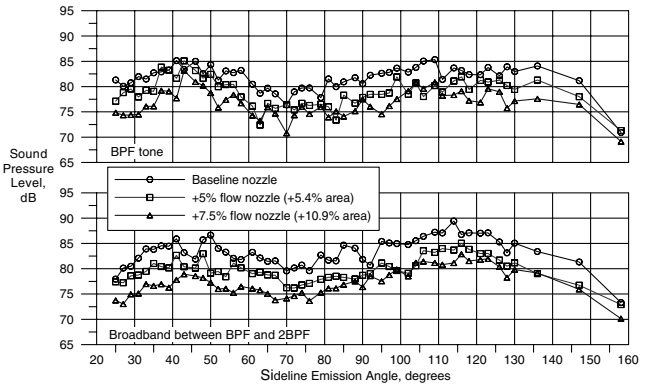

Fig. 9 Sound pressure level directivities at 61.7% design fan speed (approach condition, 89 in. sideline, no barrier wall, 59 Hz bandwidth).

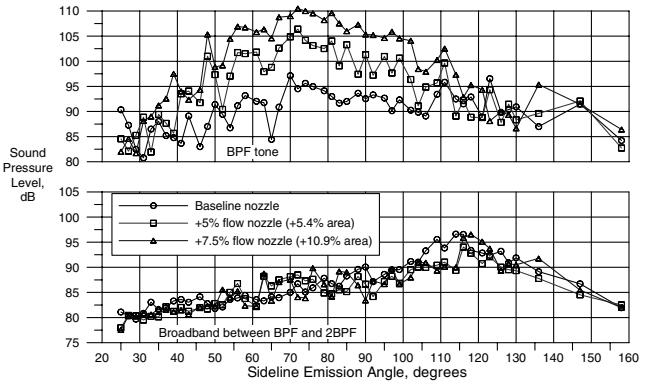

Fig. 10 Sound pressure level directivities at 87.5% design fan speed (cutback condition, 89 in. sideline, no barrier wall, 59 Hz bandwidth).

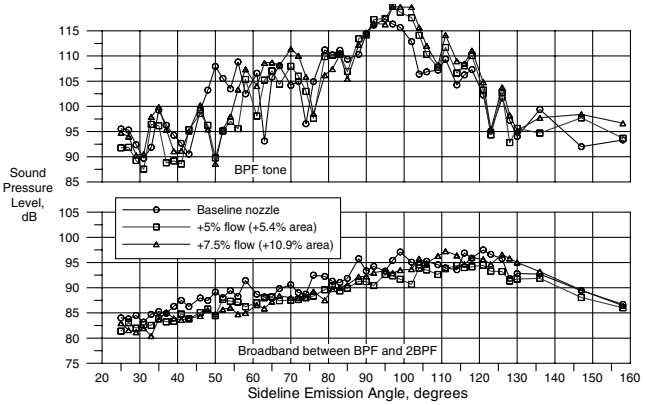

Fig. 11 Sound pressure level directivities at design fan speed (takeoff condition, 89 in. sideline, no barrier wall, 59 Hz bandwidth).

reduction with the +5% flow nozzle and 5 dB reduction with the +7.5% flow nozzle.

Rotor-alone noise begins to dominate stage noise at 87.5% speed. Increased nozzle flow at this rotor speed results in a significant increase in BPF tone level (Fig. 9), as much 15 dB at the 70 deg sideline emission angle. Also, this increased noise is not uniform over all sideline angles, but somewhat localized from 40 to 110 deg emission angles. It is possible that the BPF tone (which is just cut on at this rotor speed) is more strongly cut on with higher rotor relative velocities associated with increased nozzle flow. There is essentially no change in broadband level with increased nozzle flow at 87.5% speed.

The BPF tone level at design fan speed (Fig. 11) shows less change with nozzle flow. The BPF tone is both rotor-alone and rotor-stator interaction noise at this higher rotor speed. The representative broadband noise level between BPF and 2BPF is only slightly reduced with increased nozzle flow at design rotor speed.

D. Laser Doppler Velocimeter Results

In addition to the aerodynamic and acoustic performance data obtained during this test, flowfield velocity measurements were also made using a laser Doppler velocimeter (LDV). The LDV data were obtained to determine how the wake flow generated by the rotor changes as the nozzle area changes. These wake data can be used to explain some of the observations made above regarding how the acoustic spectra change as the nozzle area (and flow) is increased.

Figure 12 shows both a schematic of the model as it was configured during the LDV testing and the axial location at which the LDV wake surveys were conducted. Although the far-field acoustic data presented previously were obtained with the baseline radial stators installed, it was necessary to obtain the LDV data with a set of swept stators since this was the only configuration for which an LDV window was available. As can be seen in Fig. 12 the LDV data were acquired in an axial plane which intersects the leading edge of the swept stators at the hub. This axial plane also corresponds to the leading edge location of the baseline radial stators that were used during the acoustic testing. A bellmouth inlet was installed during the LDV testing, not the flight inlet (Fig. 3) used during the acoustic testing; however, model operating conditions were essentially the same as for the baseline flight acoustic configuration. LDV measurements were taken without tunnel flow since the measurements were taken within the turbofan flow passage.

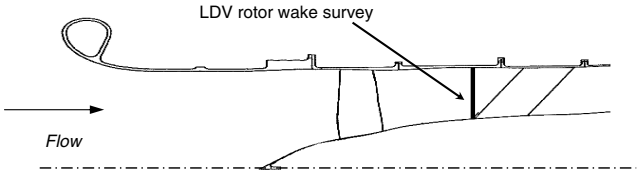

Fig. 12 Location of LDV rotor wake survey.

Figures 13 and 14 show how the rotor wake flow varies with changes in nozzle area as measured at the approach and cutback conditions, respectively. Figures 13a and 13b and 14a and 14b show that axial velocities increase and tangential velocities decrease in the rotor wake as nozzle area increases. As a result, the swirl angle also decreases (Figs. 13c and 14c). The decreased swirl suggests that the loading on the rotor blades decreases as nozzle area increases. In general, this decreased blade loading should lead to a decrease in the amount of turbulence generated by each blade. Figures 13d and 14d show that this was the case; the measured turbulence level in the rotor wake decreased as nozzle area increased. This decreased rotor wake turbulence will result in decreased levels of rotor/stator interaction broadband noise, a result which is evident in the acoustic spectra plots presented in Fig. 8. Both of these plots show a reduction in broadband noise with increasing nozzle area.

The broadband acoustic data presented for the takeoff condition in Fig. 15 show a different trend. These data are similar to the approach and cutback condition data in that they show a decrease in the broadband level as the nozzle area is increased from 0 to +5.4% open, but they are unlike the other data in that they show an increase in high frequency broadband noise as the nozzle area is increased further to +10.9% open. The LDV flowfield data can also be used to explain this anomaly. Figure 15 shows the variation in rotor wake flow with increasing nozzle area as measured at the takeoff condition. Like the data obtained at the two lower speeds, axial velocities increase (Fig. 15a), and both tangential velocities (Fig. 15b) and swirl

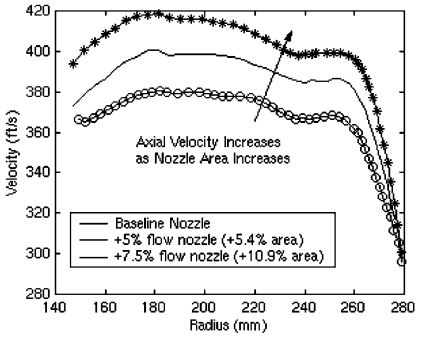

a) Mean axial velocity vs radius approach

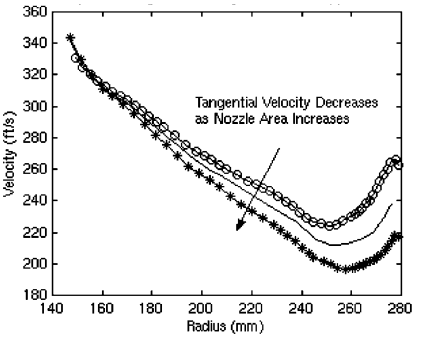

b) Mean tangential velocity vs radius approach

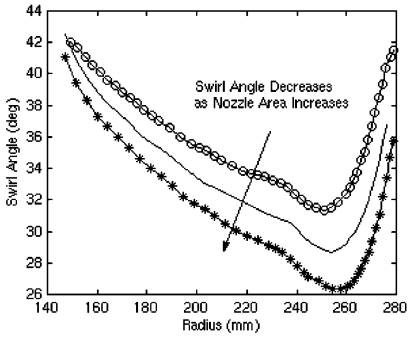

c) Swirl angle vs radius approach

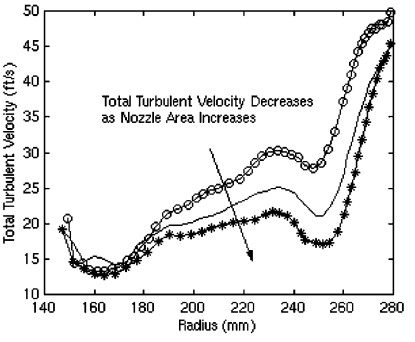

d) Mean tangential velocity vs radius approach

Fig. 13 Change in rotor wake flow with nozzle area as measured at the 61.7% design fan speed (approach condition).

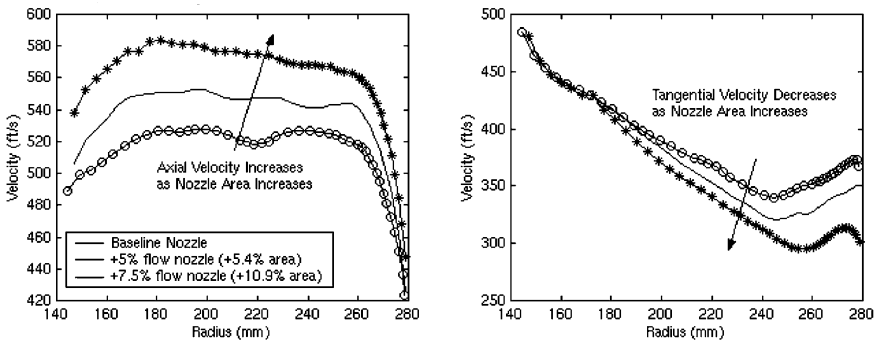

a) Mean axial velocity vs radius cutback

b) Mean tangential velocity vs radius cutback

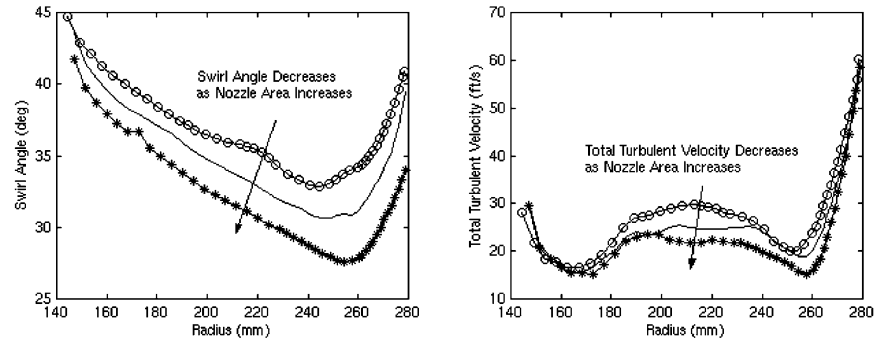

c) Swirl angle vs radius cutback

d) Total turbulential velocity vs radius cutback

Fig. 14 Change in rotor wake flow with nozzle area as measured at 87.5% design fan speed (cutback condition).

angles (Fig. 15c) decrease as nozzle area increases. The reduced swirl implies that the blade loading decreases with increasing nozzle area, a result that should lead to less turbulence generated by the blades. However, as indicated in Fig. 15d, the turbulence generated by the blades actually increases over much of the blade span as the nozzle area increases between +5.4 and +10.9% open (flow increase from +5 to +7.5%).

Figure 16 provides a more detailed look at the wake flows measured at the takeoff speed. The total turbulent velocity contours (defined as the square root of the sum of the squares of the standard deviations of the two velocity components measured at each point in space) presented in this figure indicate that the outer portions of the blade wakes get thicker and more turbulent as the nozzle area increases between +5.4 and +10.9%. This increased blade wake

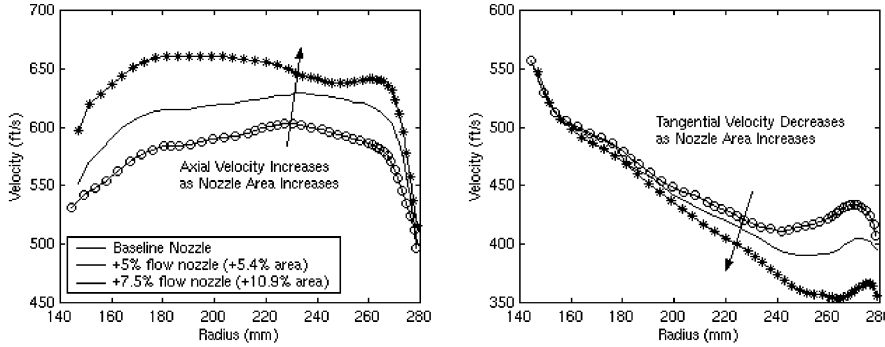

a) Mean axial velocity vs radius takeoff

b) Mean tangential velocity vs radius takeoff

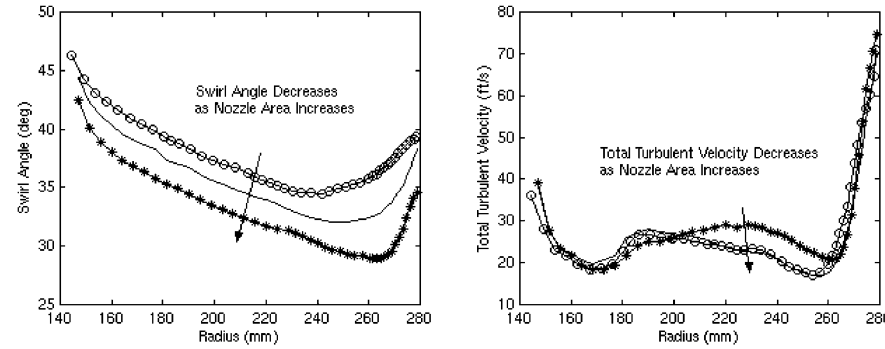

c) Swirl angle vs radius takeoff

d) Total turbulent velocity vs radius takeoff

Fig. 15 Change in rotor wake flow with nozzle area as measured at design fan speed (takeoff condition).

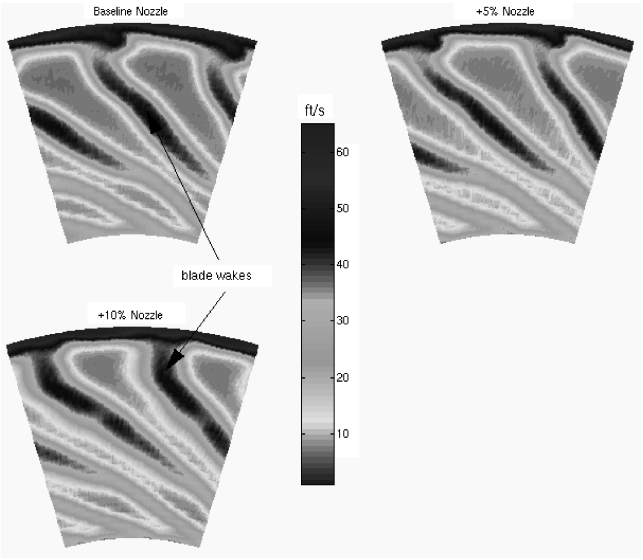

Fig. 16 Aft-looking forward view of total turbulent velocity contours measured in the rotor wake at design fan speed for each of the three nozzles (takeoff condition).

thickness may be indicating a flow separation on the rotor blades resulting, perhaps, from stronger shocks on the blades or from nonoptimum inflow angles. In any event, this increase in blade wake turbulence seems to account for the increase in high frequency broadband noise at 100% speed illustrated in Fig. 6. These thicker wakes are also consistent with the degraded aerodynamic performance measured at this test condition noted earlier in conjunction with Fig. 5. If it were not for the increased wakes near the tip, one would expect to see lower broadband noise levels when the nozzle area is increased. Because of these strong tip wakes, the broadband noise curves converge rather than decrease as nozzle area is increased.

The trends indicated by the LDV data also suggest an explanation for the increase in BPF and MPT noise which occurs when the nozzle is opened at the cutback speed. Previous reports [9,10] have presented LDV data obtained within the rotor blade passages at a radial location 0.4 in. inboard of the tip during a test in which the baseline nozzle was installed. These data show that normal shocks exist on the suction side of the blades when the fan is operating at the cutback speed. The plot presented in Fig. 15a indicates that axial flow velocities increase as the nozzle area increases from the baseline condition. The increased axial velocities would lead to higher relative flow velocities on the blades which, in turn, would be expected to lead to stronger passage shocks. The increased noise produced by these shocks is evident in the design speed acoustic spectra of Fig. 8 which show that both the BPF tone and the multiple pure tones increase as the nozzle area increases.

IV. Summary

A model turbofan was tested in the NASA Glenn 9 × 15 low speed wind tunnel at 0.1 Mach flow to investigate the effect of the variable bypass nozzle area (and flow) on the stage noise and aerodynamic performance. Test results showed that increasing the nozzle area can result in a significant noise reduction (2 EPNdB or more) while actually increasing the stage thrust and efficiency. The acoustic reduction was primarily in the broadband noise and more significant at lower fan speeds, especially at the approach condition.

Results shown in this paper suggest that a variable area bypass exhaust nozzle for a typical turbofan engine may be an effective way to further decrease engine fan stage noise and possibly realize a concurrent thrust increase. The baseline fixed-area fan nozzle in this test was sized for maximum stage performance at sea level condition. Turbofan engine bypass exhaust nozzles are typically sized for maximum performance at the portion of the aircraft flight profile where most of the flight time is spent, typically at the cruise condition. Increasing the nozzle flow within the envelope defined by desirable engine performance reduced the fan stage noise in this scale model test. Thus it may be desirable to employ a variable area engine bypass nozzle as a technique to reduce fan stage noise levels at lower rotor operating speeds by somewhat increasing the nozzle area during approach and possibly sideline conditions. Even the addition of a limited position variable area bypass nozzle, to reduce mechanical complexity and weight, might be an effective retrofit to existing turbofan engines to control fan stage noise and realize additional noise reduction without sacrificing aerodynamic performance.

References

[1] Woodward, R. P., Lucas, J. G., and Stakolich, E. G., "Acoustic and Aerodynamic Performance of a 1.83-Meter-(6-Ft-) Diameter 1.2-Pressure-Ratio Fan (QF-6)," NASA TN D-7809, Dec. 1974.

[2] Woodward, R. P., Lucas, J. G., and Balombin, J. R., "Acoustic and Aerodynamic Performance of a 1.5-Pressure-Ratio, 1.83-Meter (6-ft) Diameter Fan Stage for Turbofan Engines (QF-2)," NASA TM X-3521, April 1977.

[3] Woodward, R. P., and Glaser, F. W., "Effect of Inflow Control on Inlet Noise of a Cut-On Fan," *AIAA Journal*, Vol. 19, No. 3, March 1981, pp. 387–392.

[4] Gliebe, P. R., "The Effect of Throttling on Forward Radiated Fan Noise," AIAA Paper 79-0640, March 1979.

[5] Ginder, R. B., and Newby, D. R., "An Improved Correlation for the Broadband Noise of High-Speed Fans," *Journal of Aircraft*, Vol. 14, No. 9, Sept. 1977, pp. 844–849.

[6] Woodward, R. P., Hughes, C. E., Jeracki, R. J., and Miller, C. J., "Fan Noise Source Diagnostic Test—Far-Field Acoustic Results, AIAA Paper 2002-2427, June 2002.

[7] Hughes, C. E., "Aerodynamic Performance of Scale-Model Turbofan Outlet Guide Vanes Designed for Low Noise," AIAA Paper 2002-0374, Jan. 2002.

[8] Hughes, C. E., Jeracki, R. J., and Miller, C. J., "Fan Noise Source Diagnostic Test—Rotor Alone Aerodynamic Performance Results," AIAA Paper 2002-2426, June 2002.

[9] Podboy, G. G., Krupar, M. J., Helland, S. M., and Hughes, C. E., "Steady and Unsteady Flow Field Measurements Within a NASA 22 Inch Fan Model," AIAA Paper 2002-1033, Jan. 2002.

[10] Podboy, G. G., Krupar, M. J., Hughes, C. E., and Woodward, R. P., "Fan Source Diagnostic Test—LDV Measured Flow Field Results," AIAA Paper 2002-2431, June 2002.

[11] Heidelberg, L. J., "Fan Noise Source Diagnostic Test—Tone Model Structure Results," AIAA Paper 2002-2428, June 2002.

[12] Dahl, M. D., and Woodward, R. P., "Comparison Between Design and Installed Acoustic Characteristics of the NASA Lewis 9-by 15-Foot Low Speed Wind Tunnel Acoustic Treatment," NASA TP-2996, April 1990.

[13] Dahl, M. D., and Woodward, R. P., "Background Noise Levels Measured In the NASA Lewis 9- by 15-Foot Low Speed Wind Tunnel," NASA TP-3274, Nov. 1992.

[14] Woodward, R. P., and Dittmar, J. H., "Background Noise Levels Measured in the NASA Lewis 9- by 15-Foot Low-Speed Wind Tunnel," NASA TM-106817; also AIAA 95-0720, Jan. 1995.

[15] Woodward, R. P., and Hughes, C. E., "Noise Benefits of Increased Fan Bypass Nozzle Area," AIAA 2005-1201; also NASA TM-2004-213396, Jan. 2005.

[16] Woodward, R. P., Hughes, C. E., and Podboy, G. G., "Aeroacoustic Analysis of Fan Noise Reduction with Increased Bypass Nozzle Area," AIAA 2005-3075, May 2005; also NASA TM-2005-213825.

[17] Tyler, J. M., and Sofrin, T. G., "Axial Flow Compressor Noise Studies," *SAE Transactions*, Vol. 70, 1962, pp. 309–332.

[18] Jeracki, R. J., "Model Engine Performance Measurement from Force Balance Instrumentation," NASA TM-1988-208486; also AIAA 98-3112, July 1998.

[19] Chestnutt, D., "Flight Effects of Fan Noise," NASA CP-2242, Jan. 1982.